scientific reports

Check for updates

OPEN

Comparative of OCT and OCTA parameters in patients with early chronic angle-closure glaucoma and early pituitary adenoma

Zhi Tan[1], Kai-lun Lu[2], Wan-cheng Zhang[2], Shu-ying Peng[1], Xiu-juan Wen[2], Tong-tong Dai[2] & Yan-hua Pang[2]✉

Optical coherence tomography (OCT) and optical coherence tomography angiography (OCTA) have the potential application in evaluating pathological structural change of the optic nerve. We aimed to evaluate the value of the OCT and OCTA parameters of the optic disk and macular in differentiating early chronic primary angle-closure glaucoma (CPACG) and early pituitary adenoma (PA) in case of mild visual field defects (the mean defect (MD) > 6 dB). The results showed that regarding OCTA parameters, CPACG patients had lower retinal blood flow density of most layers of the optic disk and macular than PA patients. Regarding OCT parameters, CPACG patients had thinner circumpapillary retinal nerve fiber layer (CP-RNFL) in all quadrants and average CP-RNFL, ganglion cell layer (GCL) and macular ganglion cell complex (GCC) in each quadrant of macular inner and outer rings, and inner plexus layer (IPL) of macular inner ring, superior-outer ring and temporal-outer ring than PA patients. The Z test indicated that OCTA parameters and OCT parameters had similar value in the diagnosis of disease. In conclusion, in the case of similar visual field damage, early CPACG patients have smaller blood flow density and thinner optic disk and macular than early PA. OCTA has similar performance to OCT in diagnosing CPACG and PA.

Keywords Chronic primary angle-closure glaucoma (CPACG), Pituitary adenoma (PA), Optical coherence tomography angiography (OCTA), Optical coherence tomography (OCT)

Glaucoma is a progressive structural optic neuropathy characterized by progressive thinning of retinal nerve fiber layer (RNFL) and optic disc depression and is the second leading cause of blindness in the world[1]. In the two types of glaucoma, although the incidence of primary angle-closure glaucoma (PACG) is lower than that of primary open-angle glaucoma (POAG), but the blindness rate is high, and more than 80% occur in Asia[2,3]. Improving the diagnosis rate in order to promptly treat and slow or avoid blindness is of great significance for PACG patients, especially for patients with highly concealed chronic PACG (CPACG), a type of PACG characterized by chronic elevation of intraocular pressure. However, CPACG and intracranial optic nerve compression disease are confused in the routine diagnosis. Clinical observation points out that intraocular pressure (fluctuating changes)[4], visual field, optic disc characteristics (such as cup enlargement and RNFL thinning)[5,6], and narrow anterior chamber angle of CPACG patients overlap with these characteristics in patients with pituitary adenoma (PA). Therefore, misdiagnosis of these two diseases often occurs even among experienced ophthalmologists[7].

In recent years, combined macular Optical coherence tomography (OCT) and Optical coherence tomography angiography (OCTA) have also been applied to evaluate the damage to the macular area and optic nerve structure in glaucoma, such as the degree of visual impairment and visual field defect[8,9], aiming to provide a basis for the diagnosis and treatment of glaucoma. OCT quantitatively, objectively, and reproducibly analyzes the optic nerve fiber and the structure of the macular area in vivo via common parameters including CP-RNFL, macular ganglion cell layer (GCL), macular ganglion cell complex (GCC) layer, etc., which are used to assist diagnosis and monitoring of glaucoma[10]. OCTA is a new imaging technology that shows the RNFL and macular microvascular changes in various optic neuropathies, such as in glaucoma, and ischemic and inflammatory optic nerves[9,11]. OCTA has also been used to assess PA-induced optic nerve damage. For example, Ben Ghezala, I et al. used OCTA to

[1]Radiology Department. Affiliated Hospital of Guangdong Medical University, Zhanjiang, Guangdong Province, China. [2]Ophthalmology Department Affiliated Hospital of Guangdong Medical University, No. 57, South Renmin Avenue, Xiashan District, Zhanjiang 524023, Guangdong Province, China. ✉email: pang1049371818@163.com

follow up on the changes of radial peripapillary capillaries plexus (RPCP) vessel density in the optic disk of PA patients after optic chiasm decompression[12]. In addition, few studies have used OCT and OCTA parameters to evaluate the changes in vessel density around the optic disk and macula after optic chiasm decompression in PA patients[13,14]. These studies indicate the potential application of OCT and OCTA in the study of structural change of the optic nerve. We raise the question of whether there is a difference in OCTA blood flow density between the eyes with early PA with mild compression of the optic chiasm and early CPACG, and whether these differences in OCT and OCTA parameters of the optic disk and macula region provide objective parameters for differentiating PA from glaucoma. Therefore, in this study, we used OCT and OCTA to measure parameters of the optic disk and macular area in early CPACG and early PA patients with mild visual field defects (the mean defect (MD) > 6 dB) to evaluate the efficacy of OCT and OCTA in differentiating early CPACG from early PA. To the best of our knowledge, this is the first study to compare fundus parameters between early CPACG and early PA.

Results

Baseline information

Case group 1 included 28 patients (28 eyes), including 14 males and 14 females, with an average age of (62.857 ± 10.848) years. Case group 2 included 30 patients (30 eyes), including 13 males and 17 females, with an average age of (59.300 ± 6.114) years. The composition of PA patients in case group 2 consisted of 1 adrenocorticotropic adenoma, 1 gonadotroph adenoma, 1 prolactinoma, 1 mixed growth hormone cell and prolactinoma, and the remaining non-secretory adenomas. All 30 patients in case group 2 had grade 1 optic chiasm compression. The 29 healthy controls included 16 males and 13 females, with an average age of (59.069 ± 6.823) years. No significant difference in age and gender existed among the three groups (X2 = 0.83, P > 0.05). Best-corrected visual acuity (BCVA) was significantly lower in patients with early CPACG than in PA patients and controls, while BCVA was not significantly different between PA patients and controls (Fig. 1). Regarding IOP comparisons, patients with early CPACG were significantly higher than PA patients and controls, and the PA patients were not statistically different from the controls. Regarding the comparison of MD values, no significant difference in MD existed between the two case groups, but that of the case groups was significantly higher than that of the controls (Table 1).

Comparison of OCTA parameters between case groups and control group

Except for the SVP layer of the optic disk, the retinal blood flow density of the optic disk and macular area in early CPACG patients was smaller than that in PA patients (Table 2). Compared with the controls, the blood flow density of all layers of the optic disk and macular area in early CPACG patients decreased except for DCP, DVC and ICP of the optic disk and the optic disc SVP was smaller than the controls (Table 2).

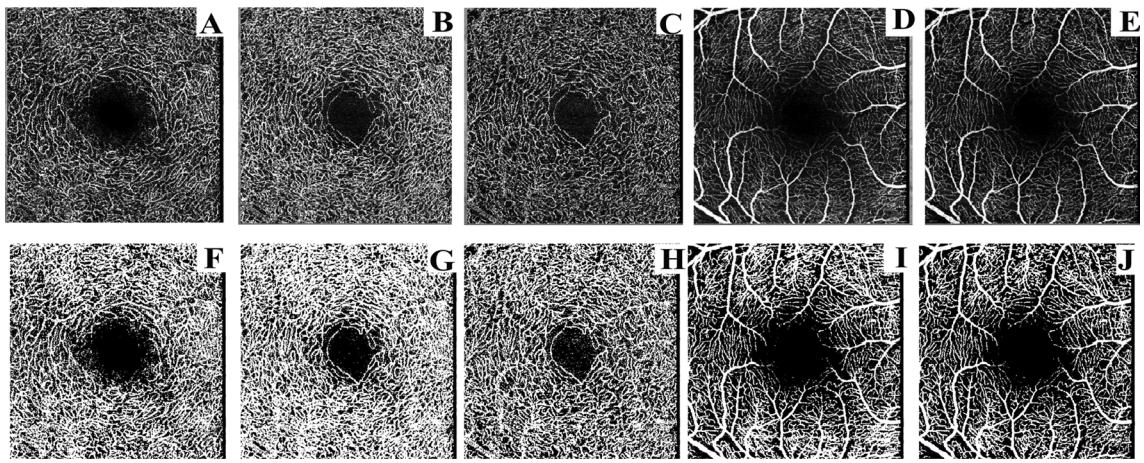

Fig. 1. (**A**–**J**) VD raw images (**A**–**E**) and VD binary images (**F**–**J**) of each layer of the macular area: A and F: DCP layer B and G: DVC layer. Cand H: ICP layer. D and I: SVC layer. E and J: SVP layer.

	Case group1 (28 eyes)	Case group2 (30 eyes)	Control group (29 eyes)	F	*P*	P_{1-2}	P_{1-3}	P_{2-3}
BCVA (LogMAR)	0.407 ± 0.295	0.103 ± 0.118	0.117 ± 0.110	12.657	0.000*	0.000*	0.000*	0.782
MD (dB)	− 2.157 ± 1.940	− 1.953 ± 2.091	− 0.169 ± 0.071	12.694	0.000*	0.639	0.000*	0.000*
Age	62.857 ± 10.848	59.300 ± 6.114	59.069 ± 6.823	1.937	0.151	0.100	0.083	0.913
IOP (mmHg)	22.964 ± 7.366	16.700 ± 2.306	15.241 ± 2.487	22.418	0.000*	0.000*	0.000*	0.229

Table 1. Comparison of general data between case groups and control group. Case group 1 represents early CPACG patients. Case group 2 represents newly diagnosed PA patients.

Macular and optic disc OCTA parameters (%)	Case group1 (28 eyes)	Case group2 (30 eyes)	Control group (29 eyes)	F	*P*	P_{1-2}	P_{1-3}	P_{2-3}
Macular DCP	15.251 ± 6.501	23.382 ± 4.343	21.259 ± 5.921	11.647	0.000*	0.000*	0.001*	0.229
Macular DVC	16.926 ± 6.262	26.307 ± 4.254	24.059 ± 5.891	16.418	0.000*	0.000*	0.000*	0.193
Macular ICP	13.382 ± 5.838	21.746 ± 4.171	20.331 ± 5.770	14.891	0.000*	0.000*	0.000*	0.392
Macular SVC	13.005 ± 5.511	20.833 ± 6.698	22.589 ± 6.529	13.915	0.000*	0.000*	0.000*	0.368
Macular SVP	17.312 ± 7.291	27.821 ± 6.692	28.582 ± 8.628	14.496	0.000*	0.000*	0.000*	0.746
Optic disc DCP	8.248 ± 4.845	11.531 ± 4.438	9.215 ± 4.079	4.183	0.019*	0.006*	0.415	0.050
Optic disc DVC	10.352 ± 4.257	13.824 ± 4.691	12.083 ± 4.693	3.054	0.049*	0.016*	0.223	0.220
Optic disc ICP	11.637 ± 4.221	15.459 ± 4.284	14.154 ± 4.795	4.018	0.023*	0.006*	0.071	0.345
Optic disc SVC	21.061 ± 10.856	32.295 ± 7.043	34.133 ± 9.776	11.994	0.000*	0.000*	0.000*	0.527
Optic disc SVP	18.412 ± 6.940	20.132 ± 3.808	24.316 ± 6.258	5.704	0.005*	0.325	0.002*	0.023*
Optic disc RPCP	21.642 ± 12.890	35.667 ± 6.641	37.33 ± 9.994	15.091	0.000*	0.000*	0.000*	0.597

Table 2. Comparison of retinal OCTA parameters between case groups and control group (%). Case group 1 represents early CPACG patients. Case group 2 represents newly diagnosed PA patients.

Comparison of OCT parameters between case groups and control group

The thickness of CP-RNFL in each quadrant and average CP-RNFL thickness in early CPACG patients was thinner than those in PA patients. Compared with PA patients, early CPACG patients had thinner GCL and GCC layers in each quadrant of the macular inner ring and outer ring, and thinner IPL layer of the each quadrant of the macular inner ring, superior region of the macular outer ring and temporal region. Compared with the control group, the average CP-RNFL and CP-RNFL in each quadrant were thinner in patients with early CPACG, while there was no significant change in CP-RNFL thickness in PA patients (Fig. 2). Regarding macular region, compared with the controls, early CPACG patients had thinner GCL and GCC layers of each quadrant of the inner and outer ring and the IPL layers of each quadrant of the inner ring, and PA patients had thinner GCL and GCC layers of nasal region of the inner ring. The GCL, IPL and GCC layers of 1 mm macular center were not significantly different among the three groups (Table 3).

Comparison of OCT and OCTA parameters in diagnostic test performance

To evaluate the diagnostic ability of OCT and OCTA parameters, we calculated the receiver operating characteristic curve (ROC) of some OCT and OCTA parameters in early CPACG and PA patients, respectively, and the ROC area under the curve (AUC) in Fig. 3. We described the parameters with relatively large AUC values as follows. The AUC of CP-RNFL thickness in the superior and inferior were 0.807 and 0.844, respectively (Fig. 3A), that of the GCL and GCC in the nasal region of the macular inner ring was 0.878 and 0.875 (Fig. 3B), that of GCC and GCL in the macular outer ring were 0.819 and 0.814, respectively (Fig. 3C) and that of the optic disk SVC and macular SVC was 0.840 and 0.889, respectively (Fig. 3D). Z-test showed that the comparison of AUC of maximum OCT parameters and OCTA parameters showed no statistical significance between the two groups ($Z_{\text{optic disc inferior CP-RNFL}} - {}_{\text{optic disc SVC}} = -0.044$, P = 1.035; $Z_{\text{optic disc inferior CP-RNFL}} - {}_{\text{macular SVC}} = -0.504$, P = 1.386; $Z_{\text{GCL of nasal inner ring}} - {}_{\text{optic disc SVC}} = 0.426$, P = 1.329; $Z_{\text{GCL of nasal inner ring}} - {}_{\text{macular SVC}} = 0.123$, P = 0.901). In PA patients, the AUC of optic disc SVP was 0.760, and the AUC of GCL and GCC in macular inner ring nasal region were 0.673 and 0.637, respectively. Z test showed that there was no statistically significant difference between any two

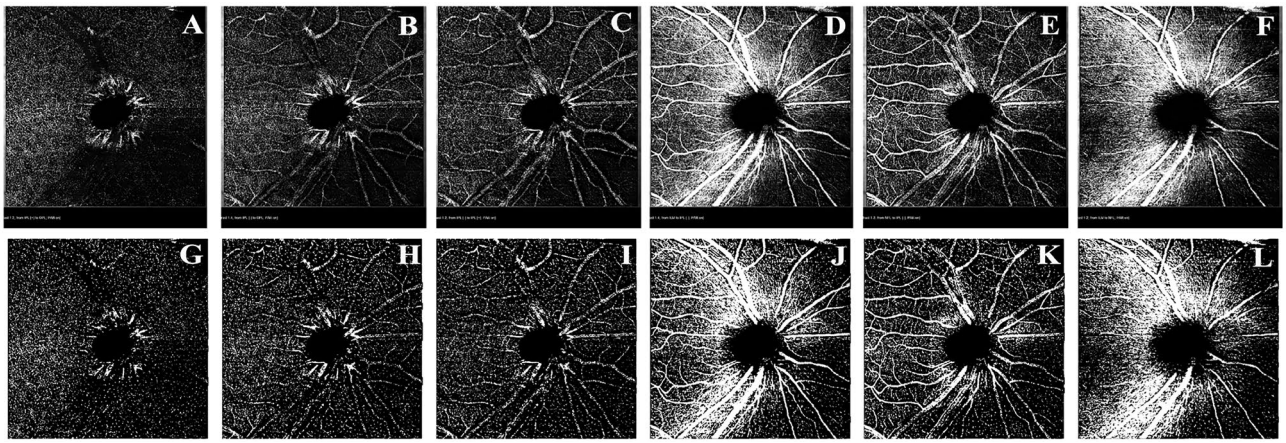

Fig. 2. (**A**–**L**) VD raw images (**A**–**F**) and VD binary images (**G**–**L**) of each layer of the optic disk: A and G: DCP layer B and H: DVC layer. C and I: ICP layer. D and J: SVC layer. E and K: SVP layer. F and L: RPCP layer.

OCT parameters (μm)	Case group1 (28 eyes)	Case group2 (30 eyes)	Control group (29 eyes)	F	*P*	P_{1-2}	P_{1-3}	P_{2-3}
Average CP-RNFL	82.303 ± 33.624	108.933 ± 11.614	108.284 ± 6.989	15.426	0.000*	0.000*	0.000*	0.904
Nasal CP-RNFL	62.892 ± 31.458	78.833 ± 15.258	79.034 ± 11.794	5.491	0.006*	0.005*	0.005*	0.971
Supra CP-RNFL	98.357 ± 45.720	133.333 ± 18.864	131.344 ± 13.672	12.838	0.000*	0.000*	0.000*	0.795
Temporal CP-RNFL	65.928 ± 25.605	83.466 ± 14.618	80.655 ± 11.796	7.665	0.001*	0.000*	0.003*	0.554
Inferior CP-RNFL	102.035 ± 44.637	140.366 ± 17.848	142.103 ± 14.283	17.839	0.000*	0.000*	0.000*	0.816
Macular GCL, IPL, and GCC thickness								
Nasal-inner ring								
	39.785 ± 10.601	47.766 ± 7.074	51.586 ± 3.727	14.557	0.000*	0.000*	0.000*	0.013*
	36.250 ± 6.107	40.633 ± 3.736	42.275 ± 2.962	13.968	0.000*	0.000*	0.000*	0.159
	94.892 ± 18.369	108.833 ± 12.793	113.517 ± 7.048	13.145	0.000*	0.000*	0.000*	0.044*
Supra-inner ring								
	43.571 ± 11.406	51.600 ± 5.340	52.103 ± 4.177	11.345	0.000*	0.000*	0.000*	0.799
	36.285 ± 6.491	40.666 ± 3.187	41.275 ± 2.877	10.636	0.000*	0.000*	0.000*	0.601
	101.821 ± 20.367	117.133 ± 9.412	117.379 ± 9.025	11.837	0.000*	0.000*	0.000*	0.946
Temporal-inner ring								
	36.821 ± 10.694	47.233 ± 6.628	46.931 ± 4.174	20.028	0.000*	0.000*	0.000*	0.870
	35.392 ± 6.436	41.033 ± 2.953	41.172 ± 2.619	16.626	0.000*	0.000*	0.000*	0.902
	89.821 ± 16.913	105.466 ± 7.700	104.655 ± 6.677	17.377	0.000*	0.000*	0.000*	0.783
Inferior-inner ring								
	42.107 ± 9.507	49.766 ± 7.285	51.137 ± 6.220	11.168	0.000*	0.000*	0.000*	0.499
	35.321 ± 5.869	39.600 ± 4.263	40.724 ± 3.411	10.878	0.000*	0.001*	0.000*	0.351
	98.857 ± 17.667	112.933 ± 13.763	115.448 ± 12.055	10.612	0.000*	0.000*	0.000*	0.511
Nasal-outer ring								
	36.285 ± 7.117	40.466 ± 4.754	41.103 ± 3.177	7.094	0.001*	0.003*	0.001*	0.642
	30.892 ± 5.065	30.000 ± 3.600	31.206 ± 3.783	0.544	0.582	0.317	0.778	0.469
	104.071 ± 18.086	117.100 ± 13.483	118.655 ± 11.162	8.709	0.000*	0.001*	0.000*	0.681
Supra-outer ring								
	30.535 ± 6.833	35.833 ± 4.202	35.620 ± 3.016	10.619	0.000*	0.000*	0.000*	0.868
	27.285 ± 3.441	29.633 ± 3.123	26.896 ± 2.857	6.544	0.002*	0.006*	0.642	0.001*
	87.892 ± 17.499	103.166 ± 10.379	101.862 ± 9.046	12.555	0.000*	0.000*	0.000*	0.696
Temporal-outer ring								
	28.250 ± 8.605	37.633 ± 4.262	37.000 ± 4.017	22.122	0.000*	0.000*	0.000*	0.684
	28.678 ± 4.675	33.866 ± 2.750	28.965 ± 4.221	16.076	0.000*	0.000*	0.784	0.000*
	74.785 ± 13.436	91.300 ± 7.679	85.137 ± 6.838	21.351	0.000*	0.000*	0.000*	0.017*
Inferior-outer ring								
	28.000 ± 6.091	33.766 ± 3.430	34.448 ± 3.660	17.445	0.000*	0.000*	0.000*	0.564
	26.285 ± 3.241	28.066 ± 2.935	27.448 ± 2.873	2.585	0.081	0.270	0.150	0.433
	83.535 ± 16.782	99.233 ± 10.695	101.793 ± 10.097	16.937	0.000*	0.000*	0.000*	0.445
Central macula (within 1 mm diameter)								
	12.357 ± 5.806	14.733 ± 8.464	12.827 ± 3.536	1.167	0.316	0.155	0.779	0.249
	17.214 ± 4.003	18.633 ± 5.235	17.689 ± 3.048	0.860	0.427	0.203	0.671	0.392
	39.714 ± 12.174	44.933 ± 16.107	41.344 ± 8.303	1.300	0.278	0.120	0.628	0.279

Table 3. Comparison of OCT parameters between case groups and control group.

groups ($Z_{SVP\text{-}GCL} = -0.910$, P = 1.637; $Z_{SVP\text{-}GCC} = -1.268$, P = 1.801). These data suggest that OCTA parameters and OCT parameters have similar diagnostic efficacy for early CPACG and PA patients.

Discussion

Despite the different pathogenesis of CPACG and PA, patients with both diseases show impaired retinal circulation and structural thinning of the RNFL. Jo Y.H. et al.[15] and Wang X. et al.[16] found that persistently elevated IOP in PACG patients may have adverse effects on retinal circulation and induce retinal ischemic damage, leading to retinal VD loss and RNFL thickness reduction. Many possible mechanisms for visual acuity and visual field damage after the compression of the optic chiasm by PA tumors were proposed[17], including ischemic damage, demyelinating lesions, retrograde degeneration, and anterograde degeneration, which are manifested as the thinning of the GCC layer in the retina, which has been confirmed by previous studies including our previous

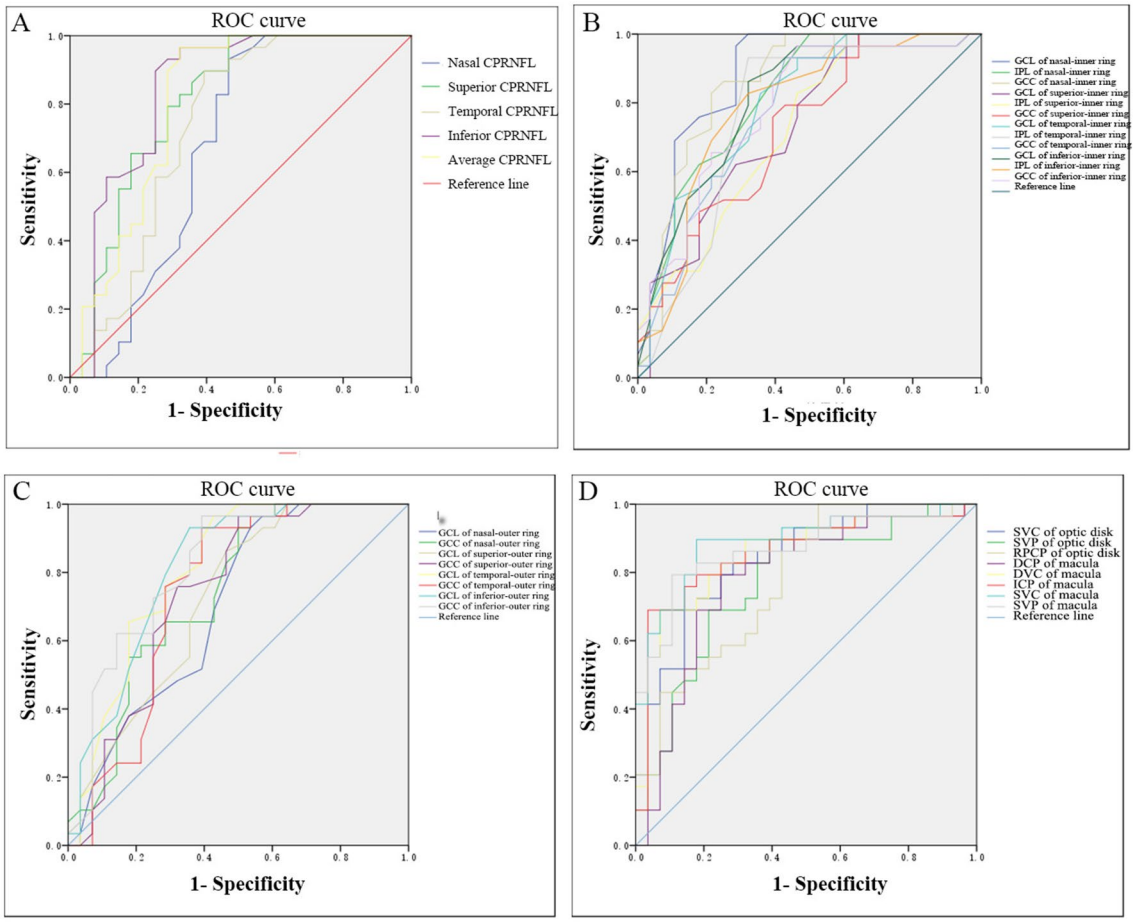

Fig. 3. AUC area under ROC of OCT and OCTA parameters in early CPACG and PA patients. (**A**) AUC area under ROC of CP-RNFL thickness in each quadrant in CPACG patients. (**B**, **C**) AUC area under the ROC curve of the thickness of the GCL, IPL, and GCC layers in each quadrant of the macular inner ring (**B**) and the GCL and GCC layers in each quadrant of the macular outer ring (**C**) in CPACG patients. (**D**) AUC area under the ROC curve of the thickness of the SVP, SVC and RPCP of the optic disk, and DCP, DVC, ICP, SVC, and SVP of macula in CPACG patients.

study[18,19]. A study using OCTA measurement found that the density of RPCP and superficial capillary plexus in the macular area of PA patients was reduced[20], which was presumed to be due to the tumor growth compressing the optic chiasm, leading to axoplasmic transport block and blood pressure supply reduction, and finally manifested as retinal vascular atrophy. Regarding the differences in the changes in optic nerve retinal structure and blood flow between glaucoma and compressive optic neuropathy, the relevant research literature has been published recently. For example, Alon Zahavi et al. compared the differences in OCT and OCTA parameters of the optic nerve in patients with open-angle glaucoma and pituitary adenoma[21]. Kun Lei et al. studied the differences in optic nerve retinal structure and blood flow density between open-angle glaucoma and compressive optic neuropathy[22]. Eun Jung Lee et al. compared the differences in optic nerve retinal structure and blood flow density between patients with normal tension glaucoma and compressive optic neuropathy[23]. In contrast, the current study is the first to compare the structure and flow density of the optic nerve and retina between patients with early CPACG and early PA.

Our study found that compared with early PA patients, early CPACG patients had lower retinal blood flow density of each layer of the optic disk and macular area except the optic disc SVP layer and thinner average CP-RNFL, GCL and GCC layers in each quadrants of macular inner and outer ring, and IPF layer in each quadrants of macular inner, the superior and temporal regions of the macular outer ring. Our results are similar to those of previous studies, which showed that in the case of a similar degree of structural damage, the degree of retinal vascular damage in compressive optic neuropathy is less severe than that in open Angle glaucoma, especially in the macular area[22]. In a study in which a silicone balloon was implanted into the orbit of cats to mimic a growing orbital tumor, the nerve fibers were extensively demyelinated within the first week, even some fibers were even completely degenerated, and the axons were partially or completely demyelinated[24]. But after 5 weeks, many axons had remyelination despite the persistence of the orbital mass. From these findings, it can be speculated that although the demyelination of axons occurs in PA patients after the chiasm is compressed by the tumor, the whole course of the disease is slow, and many damaged axons remyelination during the disease. Based on the above literature, we speculate that part of the reason for the differences in retinal structure and blood flow

density between PA patients and PACG patients is as follows. Firstly, In PACG patients, persistently elevated IOP affects retinal blood circulation, and induces apoptosis to cause the thinning of the GCL layer and RNFL, which together lead to the reduction of retinal blood flow density. In PA, the neural axis of the compressed optic chiasm is slowly demyelinated and cooccurs with remyelination, which provides a buffer time for structural changes in the GCL. As a result, the damage of the GCL and RNFL layer is lighter than that of PACG, and the decrease of retinal oxygen demand is slow, resulting in the degree of retinal vascular atrophy also lighter. Previous studies have suggested that patients do not develop visual field defects until at least 30% of retinal ganglion cells die[17]. Our previous related studies found that the functional damage of PA eyes and the structural damage of the visual pathway seem to be matched[21], which also explains why the same degree of visual field defects, but the retinal structural damage of glaucoma is more serious. Of course, further studies are needed to confirm this phenomenon.

Our study also found that the AUC of blood flow density in PACG patients was not statistically different from the AUC of structural parameters, which is similar to the results of Rao et al.[25], but different from Lin YD et al.[26]. The reason for this may be that the average deviation of VF in our study is more similar to the conditions of the former study (< –6.0 dB versus -9.2 dB) rather than the latter study (< –6.0 dB versus –19.4 dB). Compared with functional parameters, structural parameters of advanced glaucoma are more susceptible to the floor effect[27], a phenomenon that OCT has limitations in detecting RNFL thickness thinning when retinal RNFL is rarely below 50 μm in advanced glaucoma with residual vascular tissue and glial tissue,

In our study, when VF function was mildly impaired in PA patients, the optic disc SVP became smaller and the deep retinal VD was not statistically different compared with normal controls. Our finding is similar to the results of Dallorto, L et al.[28], who found that compared with healthy eyes, the optic disc VD and macular VD of the superficial vascular plexus in PA patients were significantly reduced, and no change was found in the deep retinal VD. Our study also found that the AUC of optic disc SVP in PA patients was not statistically different from that of GCL and GCC on the nasal region of the macular inner ring, which was different from the study of Tang, Y et al.[29], who believed that the AUC of RPCP on the temporal region of the optic disk in PA patients was 0.821, which had the highest diagnostic efficiency for VF abnormalities. It can be concluded that OCTA parameters can be used as markers for evaluating nerve damage in PA. Regarding retinal structure, PA patients in our study mainly showed the thinning of GCL and GCC layers on the nasal side of the inner macular ring, which was similar to the results of a previous study that found that early PA mainly manifested as the thinning of the quadrants of GCL, IPL and GCC layers[21], especially on the nasal region of the macular[30]. In view of this phenomenon, we consider the following reasons: we know that the RNFL is composed of RGC axons, the GCL is composed of RGC cell bodies, and the IPL is composed of RGC dendrites[31]. Under normal conditions, a vertical line is drawn through the fovea, and the RNFL of the retina is divided into nasal crossing fibers and temporal non-crossing fibers. The nasal RNFL drained into the nasal and temporal sides of the optic disk. The temporal RNFL drains predominantly into the superior and inferior regions of the optic disk. The macular RNFL in nasal region belongs to crossing fibers, and its retrograde degeneration after compression can occur in the early stage, leading to RGC dysfunction and/or apoptosis, which are manifested as thinning of the macular GCL and GCC layers in the nasal region. The reasons for this phenomenon are as follows: as crossing fibers, macular RNFL in the nasal region suffers from retrograde degeneration after compression in the early stage and leads to RGC dysfunction and/or apoptosis, which are manifested as the thinning of the GCL and GCC layers in the macular of nasal region.

The limitations of this study are as follows: firstly, this study is a cross-sectional study and lacks follow-up data; secondly, this study included small sample size, only involving early CPACG and early PA patients, and did not include enough cases for stratified study, which is also the experiment we will carry out further.

In conclusion, in the case of similar visual field damage, compared with early PA eyes, the blood flow density of the optic disk and macular area in early CPACG eyes is smaller, and the thickness of the optic disk and macular area is thinner, which is considered to be related to the different pathogenesis of the two diseases. OCTA parameters have similar performance to OCT parameters in the diagnosis of early CPACG and early PA.

Material and methods

Research objects

This was a retrospective clinical case–control study. We enrolled early CPACG patients who were diagnosed in the Department of Ophthalmology (termed case group 1), and early PA patients with mild chiasmal compression who were newly diagnosed by magnetic resonance imaging and postoperative pathological examination in the Department of Neurosurgery (termed case group 2) from the Affiliated Hospital of Guangdong Medical University from March 2022 to September 2023. Twenty-nine normal subjects (29 eyes) were enrolled as the control group. The diagnostic criteria of CPACG met the following characteristics[32–34]: (1) an elevated IOP (non-contact IOP ≥ 21 mmHg); (2) a narrow synechial angle; (3) no history and no ocular signs of an acute glaucoma attack; (4) more than three cumulative clock-hours of peripheral anterior synechiae by gonioscopy; 5) glaucomatous optic neuropathy or visual field defect. Early CPACG was defined as the visual field MD values > –6 dB based on a previous study[8]. Similarly, the visual field MD values of subjects included in case group 2 were also > –6 dB. All subjects underwent best corrected visual acuity (BCVA), non-contact tonometry, visual field, optic disk, and macular OCT and OCTA examinations. The study was conducted following the tenets of the Declaration of Helsinki, all participants provided written informed consent, and the study data were approved by the ethics committee of the Affiliated Hospital of Guangdong Medical University (No. PJKT2022-145).

Inclusion and exclusion criteria for case group 1 and case group 2: (1) no previous history of intracranial disease, trauma, or intracranial surgery; no history of ocular trauma, disregard of optic nerve retinal disease, and no history of intraocular surgery; (2) no glaucoma in PA patients; (3) refractive error < ± 6.0D (spherical lens)

and < 3.00D (cylindrical lens). (4) OCT and OCTA images are clear enough for data calculation and analysis; (5) patients with unclear diagnoses of PACG and PA were excluded.

Inclusion and exclusion criteria of normal control group: (1) non-contact intraocular pressure ≤ 21 mmHg; (2) visual acuity or corrected visual acuity ≥ 0.8, refractive error < ± 6.0D (spherical) and < 3.00 D (cylindrical); (3) no previous history of intracranial disease, trauma, or intracranial surgery; (4) no history of ocular trauma, glaucoma, optic nerve retinal disease, and intraocular surgery; (5) age- and gender-matched with the case groups. (6) OCT and OCTA images are clear enough for data calculation and analysis.

Visual field examination

Visual field examination (KowaAP7000 precision visual field meter, Kowa, Japan) was performed after correction of ametropia in the case group before surgery and in the control group. Reliable visual field tests were performed twice in all subjects. Visual-field tests assessed the central 30 degrees and were considered unreliable if fixation was lost, false negative or false positive errors exceeded 20%. The MD value of the visual field was a parameter used to assess the global visual field defect.

Magnetic resonance imaging of the tumor of PA patients

All patients in the PA group underwent a head magnetic resonance plain scan and enhanced examination (Discovery MR750 3.0t, GE, USA). All patients with PA underwent postoperative pathological examination of the tumor. Tumors were graded according to the compression of the tumor on the optic chiasm[35] Grade 0 was defined as no contact between the tumor and the optic chiasm. Grade 1 was defined as contact between the tumor and the optic chiasm but no deformation of the optic chiasm surface. Grade 2 was defined as contact between the tumor and the optic chiasm, and there was deformation of the optic chiasm surface, but the suprachiasmatic cisterna was still visible. Grade 3 was defined as contact between the tumor and the optic chiasm, malformation of the upper surface of the optic chiasm, invisibility of the superior cisterna of the optic chiasm, and anencephaly. Grade 4 had brain malformations in addition to the above changes.

OCT and OCTA examination

The CP-RNFL thickness, GCC thickness, IPL and GCL thickness were measured by OCT (Heideberg Engineering Spectralis, German) by the same experienced ophthalmoscope. Scanning was performed using a swept-frequency laser source with a central wavelength of 870 nm at a rate of 8.8 frames per second with high-speed scanning resolution. The CP-RNFL thickness was collected from the center of the optic disk using the international standard diameter 3.45 mm ring mode (768A-scans). The macular area was acquired by volume scanning mode scanning frame, with the macular fovea as the center, and the scanning area was 8.8 mm × 8.8 mm (31 lines, 240 μm interval, 768A-scans). The total thickness of RNFL, GCL, and IPL was defined as GCC. Vessel density (VD) images were obtained by OCTA with High Res resolution (5.7um/ pixel), foveal as the center, and range of 3 mm × 3 mm (6 μm interval, 512A-scans). An OCTA with a range of 6 mm × 6 mm was used to obtain the peripapillary VD images at each level. The VD of the optic disk includes radial peripapillary capillaries plexus (RPCP), superfical vascular complex (SVC), (superfical vascular plexus, SVP), (intermediate capillary plexus, ICP), (deep vascular complex, DVC), deep capillary plexus (DCP); VD in the macular region included SVC, SVP, ICP, DVC, and DCP.

Image processing and analysis methods

The original VD images of SVC, DVC, SVP, ICP, and DCP of the optic disk and macular area were exported from the OCTA database (Figs. 1A–E and 2A–F), and the images were processed and calculated by Image J software (version 1.53 for Mac) in 8-bit gray scale format with image threshold set. Photographs were binarized to clearly distinguish microvessels (Figs. 1F–J and 2G–L), and then VD at different levels was calculated, which was defined as the percentage of area occupied by blood vessels in the image[36].

Statistical analysis

The final sample size was calculated by PASS software (version 23.0.3) according to the mean and standard deviation of each group in the pre-experiment. Data analysis was performed by SPSS 24.0 statistical software (SPSS Inc., Chicago, IL, USA). Continuous variables that met the normality requirements of the Shapiro–Wilk test were expressed as mean ± standard deviation (mean ± SD). Independent sample t-test was used for comparison between groups. The chi-square test was used for comparison of count data between groups. One-way analysis of variance was used to compare the parameters among three groups and multiple groups, followed by an LSD-t test for pairwise comparison. The area under the ROC curve of OCT and OCTA parameters was calculated, and the area under the ROC curve of each parameter was compared by the Z test to evaluate the diagnostic ability of OCT and OCTA parameters. $P < 0.05$ was considered statistically significant.

Data availability

The datasets generated and analyzed in this study are available from the corresponding author on reasonable request.

Received: 22 February 2024; Accepted: 26 August 2024
Published online: 13 September 2024

References

1. Wu, X. *et al.* Outcomes of chronic angle-closure glaucoma treated by phacoemulsification and endocyclophotocoagulation with or without endoscopically goniosynechialysis. *Int. J. Ophthalmol.* **15**(8), 1273–1278 (2022).
2. Tham, Y. C. *et al.* Global prevalence of glaucoma and projections of glaucoma burden through 2040: a systematic review and meta-analysis. *Ophthalmology* **121**(11), 2081–2090 (2014).
3. George, R., Panda, S. & Vijaya, L. Blindness in glaucoma: primary open-angle glaucoma versus primary angle-closure glaucoma-a meta-analysis. *Eye (Lond)* **36**(11), 2099–2105 (2022).
4. R. Sihota, An Indian perspective on primary angle closure and glaucoma, Indian J Ophthalmol 59 Suppl(Suppl1), S76–81. (2011).
5. Leung, C. K. S. *et al.* Diagnostic assessment of glaucoma and non-glaucomatous optic neuropathies via optical texture analysis of the retinal nerve fibre layer. *Nat. Biomed. Eng.* **6**(5), 593–604 (2022).
6. Wang, X. *et al.* Retinal Microvascular Alterations Detected by Optical Coherence Tomography Angiography in Nonfunctioning Pituitary Adenomas. *Transl. Vis. Sci. Technol.* **11**(1), 5 (2022).
7. Dias, D. T., Ushida, M., Battistella, R., Dorairaj, S. & Prata, T. S. Neurophthalmological conditions mimicking glaucomatous optic neuropathy: Analysis of the most common causes of misdiagnosis. *BMC Ophthalmol.* **17**(1), 2 (2017).
8. Wu, J. H. *et al.* Association of macular OCT and OCTA parameters with visual acuity in glaucoma. *Br. J. Ophthalmol.* **107**(11), 1652–1657 (2023).
9. Wong, D. *et al.* Combining OCT and OCTA for Focal Structure-Function Modeling in Early Primary Open-Angle Glaucoma. *Invest. Ophthalmol. Vis. Sci.* **62**(15), 8 (2021).
10. Mohammadzadeh, V. *et al.* Macular imaging with optical coherence tomography in glaucoma. *Surv. Ophthalmol.* **65**(6), 597–638 (2020).
11. Pujari, A. *et al.* Optical coherence tomography angiography in neuro-ophthalmology: Current clinical role and future perspectives. *Surv. Ophthalmol.* **66**(3), 471–481 (2021).
12. Ben Ghezala, I. *et al.* Creuzot-Garcher, Peripapillary Microvascularization Analysis Using Swept-Source Optical Coherence Tomography Angiography in Optic Chiasmal Compression. *J. Ophthalmol.* **2021**, 5531959 (2021).
13. Lee, G. I., Park, K. A., Oh, S. Y. & Kong, D. S. Changes in parafoveal and peripapillary perfusion after decompression surgery in chiasmal compression due to pituitary tumors. *Sci. Rep.* **11**(1), 3464 (2021).
14. Cennamo, G. *et al.* The role of OCT- angiography in predicting anatomical and functional recovery after endoscopic endonasal pituitary surgery: A 1-year longitudinal study. *PLoS One* **16**(12), e0260029 (2021).
15. Jo, Y. H., Sung, K. R. & Shin, J. W. Comparison of Peripapillary Choroidal Microvasculature Dropout in Primary Open-angle Primary Angle-closure, and Pseudoexfoliation Glaucoma. *J. Glaucoma* **29**(12), 1152–1157 (2020).
16. Wang, X., Chen, J., Kong, X. & Sun, X. Immediate Changes in Peripapillary Retinal Vasculature after Intraocular Pressure Elevation -an Optical Coherence Tomography Angiography Study. *Cur. Eye Res.* **45**(6), 749–756 (2020).
17. Danesh-Meyer, H. V., Yoon, J. J., Lawlor, M. & Savino, P. J. Visual loss and recovery in chiasmal compression. *Prog. Retin. Eye Res.* **73**, 100765 (2019).
18. Biousse, V., Danesh-Meyer, H. V., Saindane, A. M., Lamirel, C. & Newman, N. J. Imaging of the optic nerve: Technological advances and future prospects. *Lancet Neurol.* **21**(12), 1135–1150 (2022).
19. Pang, Y. *et al.* Evaluation of preoperative visual pathway impairment in patients with non-functioning pituitary adenoma using diffusion tensor imaging coupled with optical coherence tomography. *Front Neurosci* **17**, 1057781 (2023).
20. Cennamo, G. *et al.* Early vascular modifications after endoscopic endonasal pituitary surgery: The role of OCT-angiography. *PLoS One* **15**(10), e0241295 (2020).
21. Zahavi, A. *et al.* Optical Coherence Tomography Angiography for the Differentiation of Glaucoma from Pituitary Macroadenoma Related Optic Disc Measurements. *Semin. Ophthalmol.* **38**(7), 625–629 (2023).
22. Lei, K. *et al.* Comparison of the retinal microvasculature between compressive and glaucomatous optic neuropathy. *Graefes. Arch. Clin. Exp. Ophthalmol.* **261**(12), 3589–3597 (2023).
23. Lee, E. J. *et al.* Peripapillary vascular density in compressive optic neuropathy and normal-tension glaucoma: a severity-controlled comparison. *Invest. Ophthalmol. Vis. Sci.* **64**(12), 10 (2023).
24. Clifford-Jones, R. E., Landon, D. N. & McDonald, W. I. Remyelination during optic nerve compression. *J. Neurol. Sci.* **46**(2), 239–243 (1980).
25. Rao, H. L. *et al.* Diagnostic ability of peripapillary vessel density measurements of optical coherence tomography angiography in primary open-angle and angle-closure glaucoma. *Br. J. Ophthalmol.* **101**(8), 1066–1070 (2017).
26. Lin, Y., Chen, S. & Zhang, M. Peripapillary vessel density measurement of quadrant and clock-hour sectors in primary angle closure glaucoma using optical coherence tomography angiography. *BMC Ophthalmol.* **21**(1), 328 (2021).
27. Suzuki, Y. & Kiyosawa, M. Visual Acuity in Glaucomatous Eyes Correlates Better with Visual Field Parameters than with OCT Parameters. *Curr. Eye Res.* **46**(11), 1717–1723 (2021).
28. Dallorto, L. *et al.* Retinal microvasculature in pituitary adenoma patients: is optical coherence tomography angiography useful?. *Acta. Ophthalmol.* **98**(5), e585–e592 (2020).
29. Tang, Y., Liang, X., Xu, J., Wang, K. & Jia, W. The Value of Optical Coherence Tomography Angiography in Pituitary Adenomas. *J. Integr. Neurosci.* **21**(5), 142 (2022).
30. Sun, M., Zhang, Z., Ma, C., Chen, S. & Chen, X. Quantitative analysis of retinal layers on three-dimensional spectral-domain optical coherence tomography for pituitary adenoma. *PLoS One* **12**(6), e0179532 (2017).
31. Seung, H. S. & Sumbul, U. Neuronal cell types and connectivity: lessons from the retina. *Neuron* **83**(6), 1262–1272 (2014).
32. Huang, H. L., Wang, G. H., Niu, L. L. & Sun, X. H. Three-dimensional choroidal vascularity index and choroidal thickness in fellow eyes of acute and chronic primary angle-closure using swept-source optical coherence tomography. *Int. J. Ophthalmol.* **17**(1), 42–52 (2024).
33. Shang, K., Hu, X. & Dai, Y. Morphological features of parapapillary beta zone and gamma zone in chronic primary angle-closure glaucoma. *Eye (Lond)* **33**(9), 1378–1386 (2019).
34. Foster, P. J., Buhrmann, R., Quigley, H. A. & Johnson, G. J. The definition and classification of glaucoma in prevalence surveys. *Br. J. Ophthalmol.* **86**(2), 238–242 (2002).
35. Fujimoto, N., Saeki, N., Miyauchi, O. & Adachi-Usami, E. Criteria for early detection of temporal hemianopia in asymptomatic pituitary tumor. *Eye (Lond)* **16**(6), 731–738 (2002).
36. Al-Sheikh, M., Ghasemi Falavarjani, K., Akil, H. & Sadda, S. R. Impact of image quality on OCT angiography based quantitative measurements. *Int. J. Retina Vitreous* **3**, 1–6 (2017).

Acknowledgements

The authors are grateful to Quan-wen Zhao for his help with the data acquisition in this paper.

Author contributions

P. YH and T. Z contributed to the conception or design of the work. L. KL, Z. WC, Z, P. SY, W. XJ, and D. TT were responsible for data acquisition. P. YH and T. Z were responsible for data analysis, manuscript writing, and

manuscript modification and science supervision. P. YH and W. XJ were responsible for manuscript submission and revision. All authors reviewed and approved the final manuscript.

Funding

This study was supported by Science and Technology Program project of Zhanjiang (230830214544759).

Competing interests

The authors declare no competing interests.

Additional information

Correspondence and requests for materials should be addressed to Y.P.

Reprints and permissions information is available at www.nature.com/reprints.

Publisher's note Springer Nature remains neutral with regard to jurisdictional claims in published maps and institutional affiliations.